Int. J. Electrochem. Sci., 9 **(2014)** 3166 - 3180

International Journal of
ELECTROCHEMICAL
SCIENCE
www.electrochemsci.org

Preparation of PVdF-PAN-V_2O_5 Hybrid Composite Membrane by Electrospinning and Fabrication of Dye-Sensitized Solar Cells

Malaisamy Sethupathy[1], *Subbiah Ravichandran*[2], *Paramasivam Manisankar*[1,*]

[1]Department of Industrial Chemistry, Alagappa University, Karaikudi-630 003, Tamil Nadu, India
[2]Electro Inorganic Chemicals Division, Central Electrochemical Research Institute, Karaikudi 630006, Tamil Nadu, India
[*]E-mail: pms11@rediffmail.com

Received: 22 January 2014 / *Accepted:* 7 March 2014 / *Published:* 23 March 2014

A porous vanadium pentoxide (V_2O_5) nano-powder are amalgamated with the polymer electrolyte mixture of poly (vinylidene fluoride) (PVdF) and Polyacrylonitrile (PAN) fibers by electrospinning method for photovoltaic performance of PVdF-PAN-V_2O_5 dye sensitized solar cells (DSSCs). This electrospinning technique compensates the disadvantage of leakage of the liquid electrolyte in DSSCs. Before evaluating the PVdF-PAN-V_2O_5 electrospun nanofiber membrane photovoltaic performance, participating component are optimized under optimum condition. The morphology and crystal structure of electrospun PVdF-PAN-V_2O_5 are analyzed using field emission scanning electron microscopy (FESEM), X-ray diffraction (XRD) and Fourier transform infrared spectroscopy (FT-IR), and parametric study like ionic conductivity electrolyte uptake, porosity also measured. As per observation of all study, a three-dimensional network structure of nanofiber membrane which is fully interconnected with combined mesopores and macropores because of a good V_2O_5 dispersion. It is found that7 wt% V_2O_5 of PVdF-PAN-V_2O_5 electrolyte membrane has the highest ionic conductivity (7.11×10^{-2} Scm^{-1}) due to the large liquid electrolyte uptake (about 576%). The composite membranes exhibit a high electrolyte uptake of 520–576%. The porosity of membranes was efficiently improved by the creation of electrospinning technique. The PVdF-PAN-V_2O_5 based DSSCs showed an open-circuit voltage (Voc) of 0.78 V, a Fill factor of 0.72 and a Short-circuit current density (Jsc) of 13.8 mA cm^{-2} at an incident light intensity of 100 mW cm^{-2}. The photovoltaic efficiency of 7.75% is comparable to that of other reported DSSCs.

Keywords: Polyvinylidene fluoride, Polyacrylonitrile, V_2O_5, Dye-Sensitized Solar Cell, Photovoltaic performance

1. INTRODUCTION

These days regularly new technology developed every day in the term of energy conversion efficiency and energy storage devices. Particularly, energy storage is the largest challenge in the field of cell phone applications and transportation [1]. The main feature of energy storage devices is the capability of high energy efficiency and power densities with outstanding cycling property that have been the subject of significant interest [2]. The demand for a substantial development of power invention is high residual to environmental problems related with existing methods including nuclear, thermal, and hydroelectric [3]. Thus, Solar cells directly convert solar energy into electrical energy and can produce electricity without special maintenance and environmental concerns [4]. From last few decades for the same reason silicon-based inorganic solar cells is in practice, but the main drawbacks of this type of solar cell such as manufacturing costs and an unwieldy fabrication process [5]. Therefore, the groups of researchers mainly consternate on to develop a type of solar cells that consist of more simply processed and low-priced materials and they have been developed a different variety of photoelectrochemical cells that convert light to electricity [6]. Since the first report by Gratzel, dye-sensitized solar cells (DSSCs) have gained much attention [7]. The Gratzel group demonstrated that power conversion efficiency (PCE) of 12% could be obtained using a liquid electrolyte-based DSSC. Importantly, this efficiency is very close to those of amorphous silicon-based inorganic solar cells [8, 9]. But, the main drawback of DSSCs is fatalities of liquid electrolytes by leakage and/or volatilization that restricted the long-term stabilities of DSSCs [9]. To rectify this problem, the group of researchers continuously trying to develop new alternative solution to replace the liquid electrolyte such as inorganic or organic hole conductors [10], ionic liquids [11], polymer [12, 13] and gel electrolytes [14, 15] in DSSCs. Even though, the preparations of these materials are complicated and poor in mechanical strength, they cannot be used in commercial production [16], to get rid of this problem soaking the polymer membrane in an electrolyte solution has been examined [17, 18].

Therefore, the numbers of processing techniques such as, template synthesis [10], drawing [19] phase separation, electrospinning [20], etc. have been used in to preparation of the polymer membrane for polymer electrolyte. Amongst, the electrospinning methodology is simple and low-cost process in which solid fibers are produced from a polymeric fluid stream (solution or melt) delivered through a millimeter-scale nozzle. This technique was first studied by Zeleny in 1914 [21] and patented by Formhals in1934 [22]. It can be explained as; an electrical field is applied across a polymer solution and a collector, to force a polymer solution jet out from a small hole. The characteristics of fiber such as large surface area to volume ratio, flexibility, leading to low density and exceptional high pore volume and mechanical properties are depending on diameter of polymer fiber materials [23]. In recent years, an electrospinning technique has paying attention due to the huge potential that the technique presents for nanomaterials and nanotechnologies [24]. The application of electrospinning mainly has been extended in to the production of mixture of materials like two different polymers [18], polymers loaded with chromophores [25], magnetic nanoparticles [26], biomolecules [27] inorganic and organic one dimensional nanomaterials [28] etc. Moreover, a huge number of synthetic and natural polymer solutions were prepared with electrospunfibers, for example polyurethanein N,N-dimethylformamide (DMF), poly(ethyleneoxide) (PEO) in water, poly(e-caprolactone)(PCL) in acetone, and PVdF in

acetone/N,N-dimethylacetamide (DMAc) [18, 29-31]. In this present study, first times reported the preparation of electrospun PVdF-PAN-V_2O_5 - nanofibers at optimized parameters by the electro-spinning method and apply to the polymer matrix in polymer electrolytes for DSSCs. To examine the effect of organic electrolyte in electrospun PVdF-PAN-V_2O_5 nanofibers on DSSCs, explored the properties like morphology (Scanning electron microscopy (SEM), X-ray diffraction (XRD) and Fourier transform infrared (FTIR) electrolyte uptake, porosity, and ionic conductivity of the electrospun PVdF-PAN-V_2O_5 nano fiber films. Photovoltaic performances of DSSC devices using these films were also investigated.

The PVdF is considered as a good base for electrolyte due to its high dielectric constant (e = 8.4), good electrochemical stability, affinity towards liquid electrolyte solutions because of electron withdrawing fluorine atoms (-C-F) in the backbone structure and exhibits ionic conductivities in the range of 10^{-4} to 10^{-3} Scm^{-1} at room temperature [32]. The film based on PVdF exhibited higher conductivity and higher degree of crystallinity. The crystalline part of PVdF hinders the free migration of Li+ ions and hence PVdF-based electrolytes have lower evaporation. These properties of PVdF are helpful in breaking the lithium salt to lithium ions while transforming into a polymer electrolyte. Even though, PAN has attractive individuality such as thermal constancy, high-quality ionic conductivity and excellent morphology for electrolyte uptake and good compatibility with liquid electrolyte. The PAN having –CN groups that easily make bond with –C=O groups of the propylene carbonate (PC) or ethylene carbonate (EC) and also with Li+ ions [32, 33]. Literatures reported that from nuclear magnetic resonance, differential scanning calorimetry, FTIR spectroscopy studies on PAN-based electrolytes demonstrate the interactions between the groups in PC or EC and PAN [34]. Thus, the PVdF and PAN are independently having advantageous characteristics as a host polymer in polymer electrolytes. Furthermore, in a group both the polymer electrolytes are sharing few important characteristics which could not be derived from PVdF or PAN. Therefore, it can be concluded that polymer electrolytes prepared from the composites of PVdF and PAN may have the characteristics interaction advantages of both PVdF and PAN. Yin and Yang et al. [35, 36] have earlier reported that PVdF and PAN are partially miscible and the composites have an asymmetric structure. The electrospun fibrous polymer electrolyte membranes have better electrochemical properties due to their unique porous structure and exceptional porosity. On the other hand, pure polymer electrospun fibers have limited efficiency in stabilizing the DSSCs at high discharge rate due to polymer degradation and the leakage of organic liquid electrolyte because these polymer nanofiber membranes only exhibit macroporous structures (pore size > 1μm) and do not have mesoporous structures (2nm< pore < 50 nm) [33].

Among, the all reported metal oxides such as (MnO_2, V_2O_5, SiO_2, TiO_2 and RuO_2) for energy sensing applications, vanadium pentoxide (V_2O_5) shows excellent physical and chemical properties, and great potentiality towards at temperatures ranging from 147 to 68 ºC. However, V_2O_5 less studied compared to other metal oxides materials. Recently, V_2O_5 nanostructures have been planned for the monitoring of sensing, supercapacitor etc [37]. Inorganic V_2O_5 has been attracted much attention because of its high surface area and redox activity it is in the form of one-dimensional structures such as nanotubes, nanowires and nanobelts has also been successfully used to detect selective gas sensors such as ammonia, cathodes in rechargeable ion batteries [38, 39]. The structures of V_2O_5 are arranged

in layered lamellar form that shows intercalated nano-spaces which can be used as a reaction space of guest organic monomers [40, 41]. Thus, guest monomers are attacked into the V_2O_5 layered spaces and at the same time polymerized into polymers by redox reaction with V_2O_5 layers [41]. However many studies have been accomplished for V_2O_5/polymer composite structures but still untouched in internal morphology and in DSSCs application. In this study, we demonstrate the alignment of V_2O_5/PVdF-PAN nanofibers to form macroscopic structures using a DSSCs device.

2. EXPERIMENTAL

2.1. Materials

Poly(vinylidene fluoride) (PVdF), Polyacrylonitrile (PAN), vanadium pentoxide (V_2O_5), acetone, *N*, *N*-dimethylacetamide, lithium iodide, iodine, ethylene carbonate (EC), and propylene carbonate (PC), 1-Hexyl-2,3-dimethylimidazolium iodide were purchased from Aldrich Chemicals and 4-*tert*-butylpyridine from TCI Chemicals. All reagents were used without further purification and rest other reagents and solvents were commercially available and were used as received.

2.2. Preparation of electrospun nanofiber composite membrane PVdF-PAN- V_2O_5

Mixture of PVdF-PAN solution was prepared by mixing PVdF and PAN in 3:1 weight ratio and the mixture was dissolved in acetone: DMF (7:3, v/v). Then V_2O_5 was mixed with different concentration at 60 ºC for 12 hrs. The contents of V_2O_5 in the composite were 0, 3, 5, and 7 wt% based on the weight of PVdF-PAN. Further, the composite blend solution was filled in to the 10 ml stainless steel syringe (needle- 24 G) using a syringe pump (KD Scientific, model 100), with a mass flow rate of 1.5 ml h^{-1} and then after steel needle was connected to an electrode and high voltage supply of 20 kV was applied to the end of the needle. The distance between the syringe nozzle and the aluminum foil collector was kept at 15 cm at room temperature. Thus after the complete electrospinning process, the nanofibrous membrane was carefully peeled off from the aluminium foil and then collected membranes were vacuum dried at 80ºC for 12 h.

2.3. Characterization of elecrospun nanofiber composite membrane (PVdF-PAN- V_2O_5)

2.4. Morphology observation

The morphology of composite membranes was examined by a scanning electron microscopy (HRSEM) (FEI Quanta 250 Microscope, Netherland). The average diameter of nanofibers was determined by analyzing the SEM images with an image analyzing software (Gwyddion 2.28).

2.5. X-ray diffraction (XRD) and Fourier transform infrared (FTIR) analysis

The XRD measurement was carried out to characterize the crystalline phase of PVdF–PAN-V_2O_5 nanofiber membranes evaluated by computer controlled XRD system ('X' Pert PRO PAN anlytical diffractometer) with Cu Kα radiation at 40 kV/30 mA. The diffractograms were scanned in a 2θ range of 10-70 at a rate of 2 min^{-1}. Fourier transform infrared (FTIR) spectra recorded at KBr pellets using Nicolet 5700 spectrophotometer (Thermo Electron Co. USA) in the wave number range 400-4000 cm^{-1} determined the presence of functional group in PVdF-PAN- V_2O_5 electrospun nanofiber membrane.

2.6. Porosity measurements

The membrane porosity ε (%) was defined as the volume of the pores divided by the total volume of the porous membrane. It could usually be determined by gravimetric method, determining the weight of liquid contained in the membrane pores [42]. The porosity percentage of PVdF-PAN-V_2O_5 composite electropun membrane was determined using n-butanol uptake. For this purpose composite membrane was soaked in n-butanol for 2 hrs. The mass of PVdF-PAN- V_2O_5 composites membrane before and after immersion was measured. The porosity % of the membrane was calculated using the Eq. (1):

$$\varepsilon\,(\%) = \frac{(w_1 - w_2)/d_w}{(w_1 - w_2)/d_b + w_2/d_p} \times 100 \qquad (1)$$

where w_1 was the weight of the wet membrane (gm), w_2 was the weight of the dry membrane (gm), after and before soaking in n-butanol, whereas d_b and dp were density of the n-butanol, and polymer respectively

2.7. Electrolyte Permeation property measurements

To determine the electrochemical properties of the composite PVdF-PAN- V_2O_5 electrospun nanofiber was soaked in an electrolyte solution consisted of 0.6 M 1-hexyl-2,3-dimethylimidazolium iodide, 0.1 M LiI, 0.05 M I_2, and 0.5 M 4-*tert*-butylpyridine in EC/PC (1:1 wt %). The % of electrolyte uptake of the electrospun membrane was determined by soaking the membranes in liquid electrolyte solution and determined at various soaking interval. The initial weight of the dried and wetted composite membranes measured. After that, soaked membranes remove from the excess liquid electrolyte and remaining electrolyte on the surface of the membrane removed by wiping softly touch with a tissue paper. The electrolyte uptake was calculated using the Eq. 2 [43].

$$Electrolyte\ uptake\ (\%) = \frac{M_{wet} - M_{dry}}{M_{dry}} \times 100\% \qquad (2)$$

where, M_{wet} and M_{dry} are mass of membranes after and before soaking in the liquid electrolyte, respectively.

2.8. Impedance study

The ionic conductivity was calculated using the "Frequency response analyser (FRA) (Autolab PGSTAT 30, Netherlands)" by scanning from 10 mHz to 100 kHz. The electrospun PVdF-PAN- V_2O_5 composite membranes were immersed in liquid electrolyte solution consists of in 0.6 M 1-hexyl-2,3-dimethylimidazolium iodide, 0.1 M LiI, 0.05 M I_2, and 0.5 M 4-*tert*-butylpyridine in EC/PC (1:1 volume%) for 60 min. During the measurement, the electrolyte samples were sandwiched in to two stainless steel (SS) blocking electrodes (surface area: 1 cm^2). Using an FRA1260 frequency response detector the resistance of the polymer electrolyte was measured. The frequency ranged from 10 mHz to 5MHz and the ac amplitude was 10 mV at room temperature. The data was analyzed by Z-plot software. The Impedance spectrum determined the bulk resistance of the polymer electrolyte. Afterwards, the ionic conductivity was obtained using the following Eq. (3):

$$\sigma = \frac{d}{R_b S} \qquad (3)$$

Here, σ is the ionic conductivity R_b is the bulk resistance; and *d* and S are the thickness and surface area of the specimen, respectively.

2.9. Contact Angle measurements

To understand the wettability of PVdF-PAN nanofiber membrane and its V_2O_5 composites, the contact angle was measured using VCA optima, ACT product, INC. Hydrophilic or Hydrophobic characteristic natures of samples were predictable by contact angle (θ) value. The wetting liquid was Milli-pore-grade distilled water (liquid surface tension (γ1) = 72.8 $mJ \cdot m^{-2}$) [44]. A portion of membrane was placed on a platform and deionized (DI) water was used as liquid at room temperature. A micro-syringe was then used to generate the droplets (5 μL) on the membrane surface. The instrument captures a digital image of the drop on the membrane and estimates the θ by geometrical methods (sessile drop, circle-fitting, etc.). When a drop of liquid is brought into contact with a flat solid surface, the final shape taken by the drop is expressed by "θ". To reduce experimental error, the contact angles were calculated 3 times for all sample and then averaged. The increased value of cos θ denoted higher wettability characteristics of the material.

2.10. Fabrication of DSSC Devices

The fabrication of DSSCs device involved the incorporation of working electrode (TiO_2) impregnated with dyes and Pt counter-electrode. To prepare the working electrode a thin layer of nonporous TiO_2 film was deposited on cleaned FTO conducting substrate, using 5% titanium (IV) butoxide in ethanol by spin-coating at 3000 rpm. The TiO_2 paste spread on the conducting glass

substrate using a doctor blade technique followed by annealing at 450 °C. Furthermore, for preparation of the dye solution, the sensitizer N719 dye was dissolved in 0.3 mM pure ethanol solution and then the TiO_2 film was dipped in the same solvent at room temperature for 24 hrs. To minimize the moisture of TiO_2 exposed in to the ambient air, later the dye-sensitized TiO_2 electrode was rinsed with anhydrous ethanol and dried in moisture free air. Simultaneously, counter electrode was prepared using a drop of 5 mM platonic chloride solution (H_2PtCl_6) in 2-propanol and it was spread on the FTO glass, sintered at 450 ºC for 30 min followed by drying and annealing at a controlled heating rate (5 ºC/min), and then cooled down from 450 to 25 ºC at a controlled cooling rate (5 ºC/min). The DSSCs was fabricated by sandwiching a piece of electrospun PVdF-PAN-V_2O_5 polymer electrolyte between a dye-sensitized TiO_2 working and Pt counter electrode. For comparison, a reference DSSCs based on liquid electrolyte was fabricated by placing the platinum electrode over the dye-coated TiO_2 electrode. The edges of the cell were sealed with 1mm wide strips of 60 μm thick Surlyn, in order to control the thickness of the electrolyte film and to avoid the short-circuiting of the cell. A hot press was used to press together the film electrode and the counter electrode. A drop of the liquid electrolyte solution was introduced into the clamped electrodes through one of two small holes drilled in the counter electrode. The holes were then covered and sealed with small squares of Surlyn strip. The resulting cells had an active area of 0.5cm × 0.5 cm.

2.11. I-V measurement

The photovoltaic performance of the DSSCs devices were measured by using the solar simulator (150 W simulator, PEC- L11, PECCELL), under air mass 1.5 and 100 mW cm^{-2} of the light intensity. The active area of the DSSC devices measured by using a black mask was 0.5 cm^{-2}. The photoelectron-chemical parameters, i.e., the fill factor (FF) and light-to-electricity conversion efficiency (η), were calculated by the following Eq.(4 and 5):

$$FF = \frac{V_{max} \times J_{max}}{V_{oc} \times J_{sc}} \quad (4)$$

$$\eta(\%) = \frac{V_{max} \times J_{max}}{P_{in}} \times 100 = FF = \frac{V_{oc} J_{sc}}{P_{in}} \times 100 \quad (5)$$

where Jsc is the short-circuit current density (mA cm-2); Voc is the open-circuit voltage (V); Pin is the incident light power (mW cm^{-2}); and J_{max} (mA cm^{-2}) and V_{max} (V) are the current density and voltage in the I-V curves, respectively, at the point of maximum power output.

3. RESULTS AND DISCUSSION

3.1. Surface morphology of electrospun PVdF-PAN-V_2O_5 composite membranes

Figure. 1 shows the SEM images of PVdF-PAN-V_2O_5 composite membranes. The resulted nanofiber membranes exhibited fully interconnected large pore structure with uniform pore size distribution. It is important to note that there is no bead formation under the optimized conditions

preferred by us for the electrospinning. Fig.1a–1c presents the morphological structure of PVdF-PAN-V_2O_5 electrospun composite nanofiber with different V_2O_5 contents. In accumulation of V_2O_5 nanoparticles, the surface roughness increased with increasing the V_2O_5 contents.

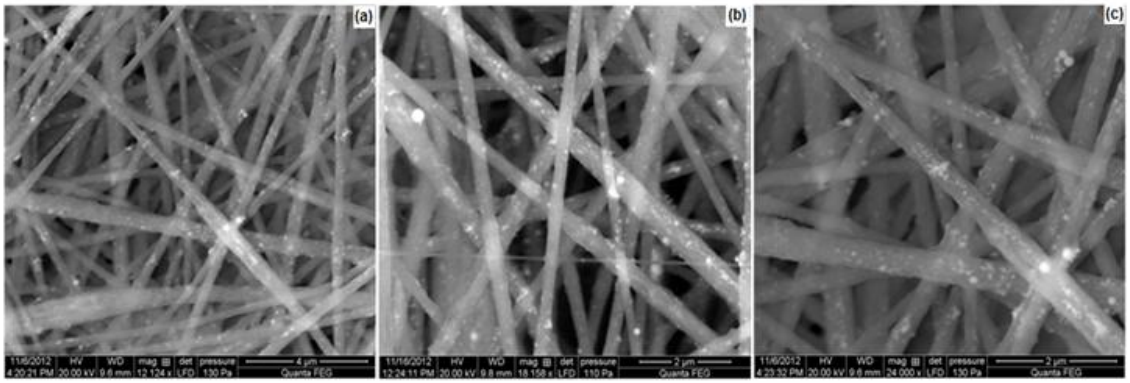

Figure 1. FE-SEM image of electrospun composite nanofiber membrane with different V_2O_5 content: (a) PVdF-PAN-V_2O_5 3wt%; (b) PVdF-PAN-V_2O_5 5 wt%; (c) PVdF-PAN-V_2O_5 7 wt%.

The average diameters of composite nanofibers for 3%, 5% and 7% V_2O_5 nanofibers are around 360, 287 and 264 nm respectively. It is clearly observed that as the V_2O_5 content is increased, the size of the fiber decreases. This may be due to incorporation of higher quantity of V_2O_5 which controls the diagonal growth of the fiber. Further increase in the content of V_2O_5 resulted in thinning of the fiber which may result in decrease in the strength. The presence of large consistent pores is apparent from the SEM image of electrospun membrane and this result in the high pore volume which is needed for a good membrane.

3.2. FTIR analysis

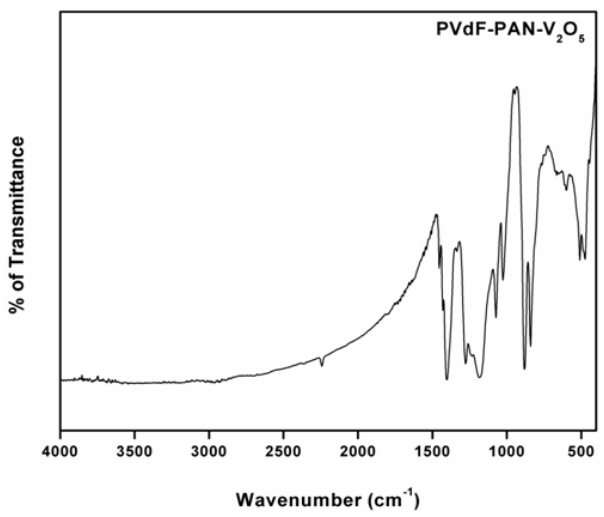

Figure 2. FT-IR spectra of PVdF-PAN-V_2O_5

The FTIR spectra were recorded for the nanofiber membranes in the range of 400-4000 cm^{-1}. Figure.2 shows, FT-IR spectrum of PVdF-PAN-V_2O_5 composite bands around 1025.38, 840 and 509, 473 cm^{-1} which corresponding to the V=O stretching vibration, V-O-V asymmetric stretching vibration, V-O-V stretching vibration and V-O-V symmetric stretching of the bond respectively. Thus, these explanations clearly show that there are molecular level interactions between the two polymers in the composite fibers [45].

3.3. XRD of composite membranes

Figure.3 shows the XRD pattern of PVdF-PAN-V_2O_5 composite membranes with various V_2O_5 contents. The XRD of electrospun PVdF-PAN-V_2O_5 membranes exhibits peaks at 20.6°, 20.2° and 20.1° respectively. The crystalline nature of electrospun PVdF-PAN-V_2O_5 composite fibers XRD measurements were performed and it shown in Fig. 3a, 3b, and 3c. The peak intensity was decreased in PVdF-PAN- V_2O_5 membrane around 20.6° for 3% of V_2O_5 was used due to the crystalline nature. But the higher percentage of V_2O_5 shows more amorphous nature. Jung et al has reported the amorphous structure has achieved when adding the highest percentage of inorganic filler was used. Due to inorganic filler was can decrease the crystallinity [44] figure 3a indicates that the crystalline eveidance of the peak at 20.6° degree becomes weak by adding more than 3wt % V_2O_5 particles. This means that the better dispersion of the mesopores and macropores V_2O_5 particles to composite solutions enhances the amorphous phase in electrospun composite membranes.

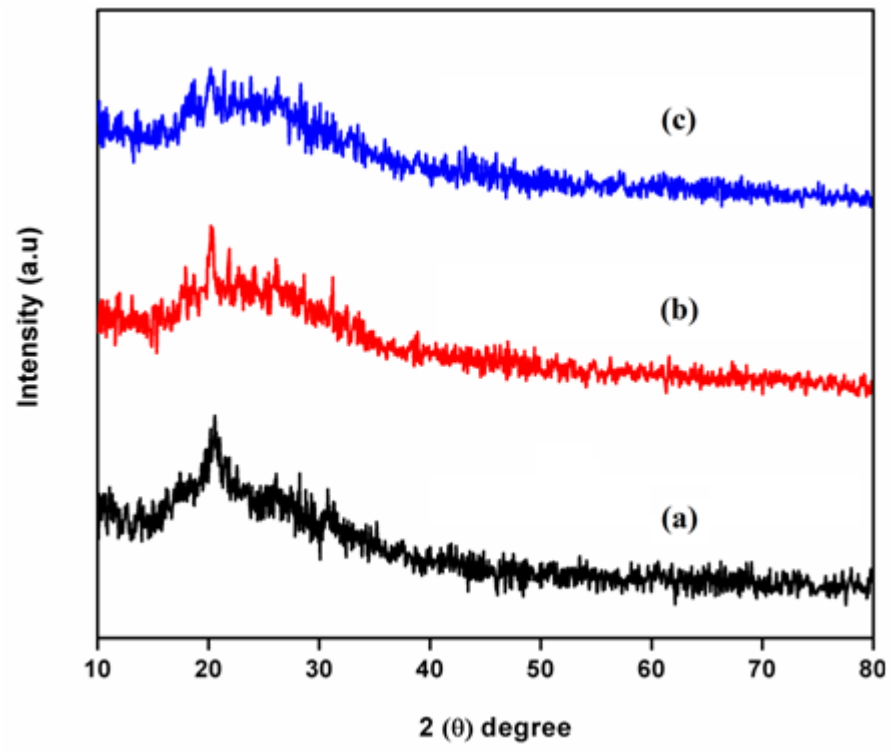

Figure 3. The XRD pattern of (a) PVdF-PAN-V_2O_5 3wt%, (b) PVdF-PAN-V_2O_5 5 wt%, (c) PVdF-PAN-V_2O_5 7 wt%

3.4. Porosity measurements and Electrolyte Permeation property

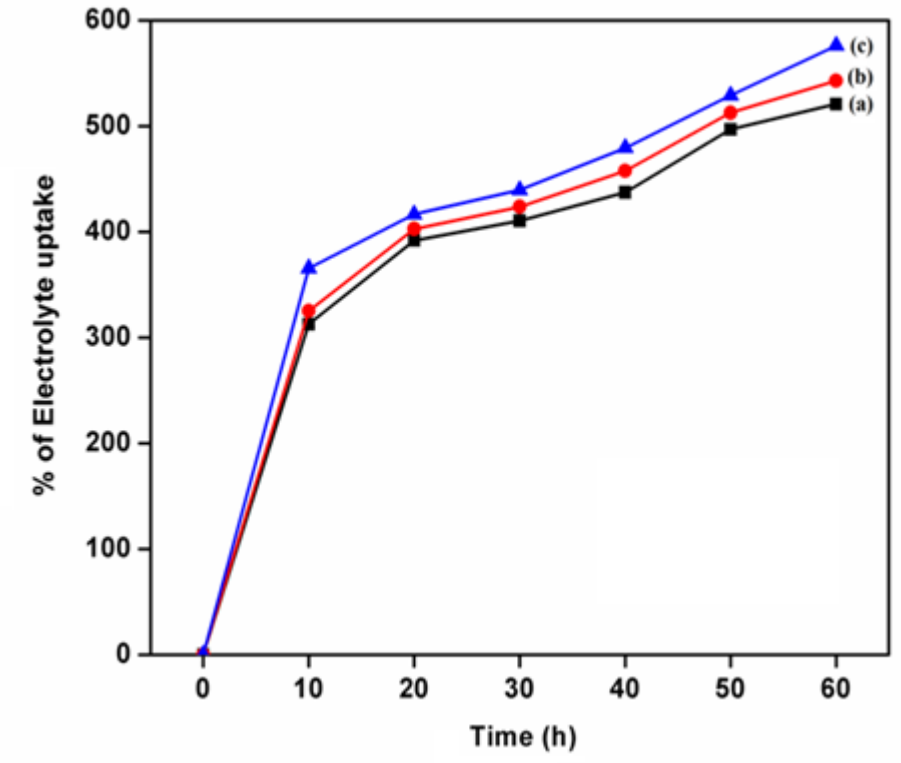

Figure 4. Electrolyte uptake characteristics of (a) PVdF-PAN-V_2O_5 3wt%; (b) PVdF-PAN-V_2O_5 5 wt%; (c) PVdF-PAN -V_2O_5 7 wt%.

Figure. 4 shows the capacity of electrolyte permeation property and porosity percentage of fiber of electrospun PVdF-PAN-V_2O_5 membranes. The average fiber diameter of electrospun membranes plays an important role in determining the membrane porosity, pore size, and specific surface area [46] and these parameters are interrelated to the electrolyte uptake of solution, electrochemical performance and its stability. Fig. 4 showed a study of the electrolyte uptake of the electrospun nanofiber membranes. The data was obtained by soaking the nanofiber membranes in the liquid electrolyte of 0.6 M 1-hexyl-2, 3-dimethylimidazolium iodide, 0.1 M LiI, 0.05 M I2, and 0.5 M 4-tert-butylpyridine in EC/PC (1:1 wt %) for a period of 1 hr. The electrolyte uptake increase steadily with increasing the V_2O_5 concentration in composite electrospun PVdF-PAN-V_2O_5 membranes. The % electrolyte uptake of PVdF-PAN-V_2O_5 fiber shows higher uptake about 576 %. Thus, the absorption of the huge amounts of liquid electrolyte by the electrospun-composite nanofiber membranes results from the high porosity of the membranes and the amorphous content of the polymer. Furthermore possibly, the completely 3D interconnected pore structure makes fast diffusion of the liquid into the membrane, and hence the uptake process is alleviated within the initial 10-20 min [47, 48].

The porosity, measured by n-butyl alcohol (BuOH) uptake, increases from 84.4 % to 85.9 % with increasing V_2O_5 concentration from 3 to 7 wt %. All samples have good porosity due to their well-developed interstices by the interwoven structure among fibers. In addition, 7 wt% composite membranes show the higher porosity by well-developed large pores/interstices on account of the

increased surface roughness. Thus, the membranes with higher degree of porosity enhance the surface area of the pore that result in the higher uptake of the electrolyte solution. Therefore, the porosity plays an important role in the electrolyte uptake process.

3.5. Impedance study

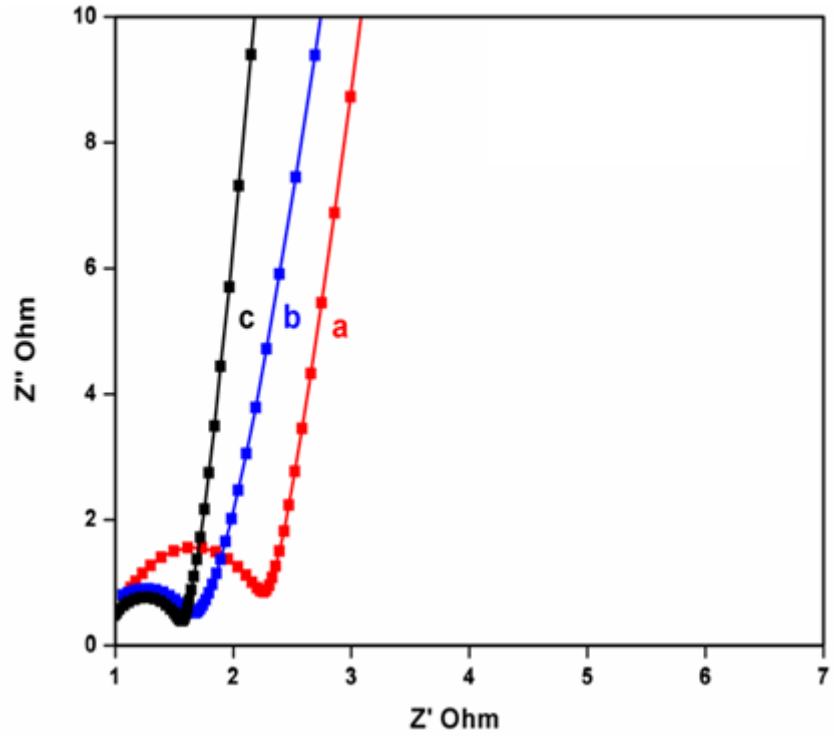

Figure 5. The ionic conductivity of (a) PVdF-PAN-V_2O_5 3wt%; (b) PVdF-PAN-V_2O_5 5 wt%; (c) PVdF-PAN -V_2O_5 7 wt%.

From the impedance data, the ionic conductivities of the nanofiber membranes at room temperature are calculated. The ionic conductivities of the electrospun-nanofiber membranes were measured at room temperature by the AC impedance method. Figure. 5a to 5c shows the AC impedance data of PVdF-PAN with V_2O_5 fillers in polymer electrolytes respectively. The ionic conductivity mainly depends on the pore structures that catch liquid electrolytes and determined the proper flow of ionic conduction [49]. The porosity, volume ratio, nature of porous polymer electrolyte and interconnectivity of membrane, determine the uptake and ion conductivity of the electrolyte [50]. The ionic conductivities of PVdF-PAN-V_2O_5 (3, 5, and 7 wt %) were $6.18\times10^{-2}Scm^{-1}$, $6.56\times10^{-2}Scm^{-1}$ and $7.11\times10^{-2}Scm^{-1}$. The higher conductivities observed are due to well interwoven structure introduced during electrospinning. Moreover, the incorporation of V_2O_5 into the electrospun nanofiber membrane improved the ionic conductivity in composite PVdF-PAN-V_2O_5. The enhancement of ionic conductivity in composite polymer electrolytes has been attributed mainly to the decreased polymer crystallinity in the presence of the inorganic particles and also to the Lewis acid-base type interactions

between the polar surface groups of inorganic particles and the ionic groups in the composite polymer electrolyte [51].

3.6. Wettability test

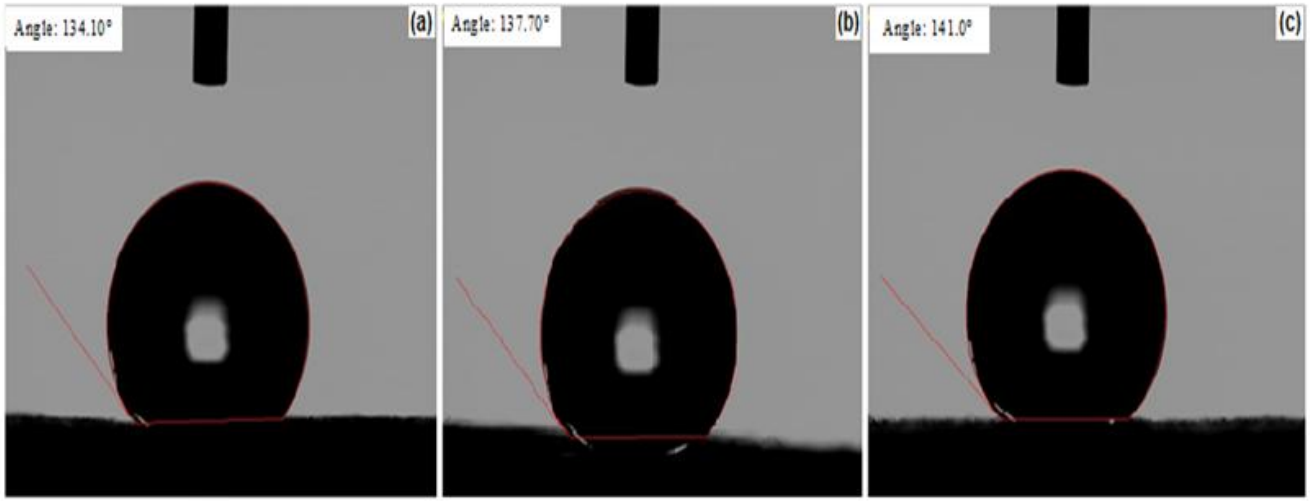

Figure 6. Contact angle measurement on (a) PVdF-PAN-V_2O_5 3wt%; (b) PVdF-PAN-V_2O_5 5 wt%; (c) PVdF-PAN -V_2O_5 7 wt%.

Contact angles are used to predict wettability and adhesion, and to indicate monolayer overage of adsorbed or deposited films. The contact angles measured for PVdF-PAN-V_2O_5 (0, 3, 5, 7% wt) composite membranes are 134.10°, 137.70° and 141.0° (Figure. 6.a-c). Since the contact angles are higher than 120°, the composites are considered to have higher hydrophobic nature. Among the composites, the composite having 7% wt V_2O_5 exhibits highest value of 141.0°. This may be due to increase in the surface roughness and the high surface area due to the incorporation of higher proportion of V_2O_5.

3.7. Photoelectric performance of DSSC with composite PVdF-PAN-V_2O_5 polymer electrolyte

The PVdF-PAN-V_2O_5 composite fibers having excellent ionic conductivity, porosity percentages and electrolyte uptake, hence they are considered to be a good quasi solid-state membrane for DSSCs. The I-V measurement curves of the DSSCs with composite PVdF-PAN- V_2O_5 polymer electrolyte were measured under irradiation of 100 mW cm^2. The I-V parameters for DSSCs such as short circuit photocurrent density (J_{sc}), open circuit voltage (V_{oc}), fill factor (FF) and the overall energy conversion efficiency (η) are presented in Table 1. The I-V graph showing the photovoltaic performances for DSSCs constructed from the composites are presented in Figure.7. The DSSCs constructed with PVdF-PAN-V_2O_5 polymer electrolytes exhibit higher photovoltaic performance. This shows the role of V_2O_5 in increasing the performance.

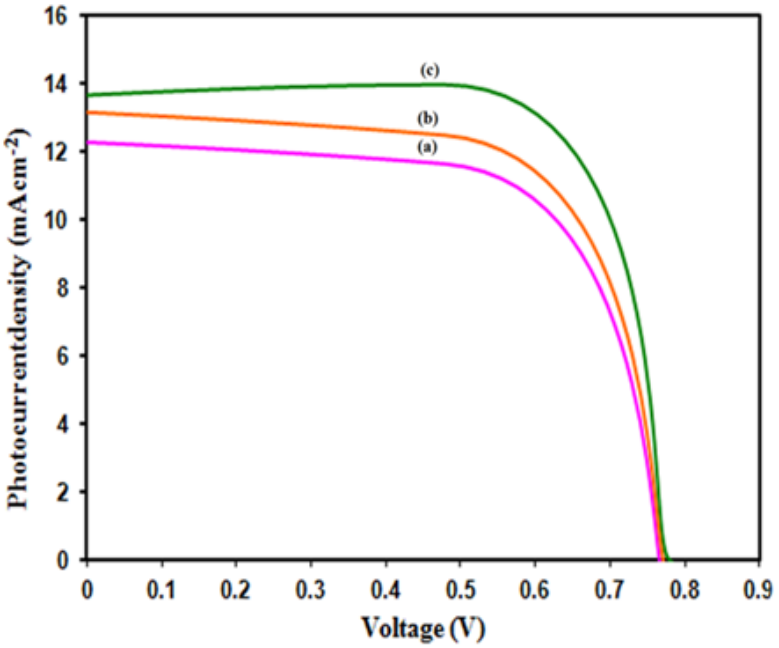

Figure 7. I-V curves of DSSCs device using electrospun PVdF-PAN-V_2O_5 nanofiber membrane

Among the PVdF-PAN-V_2O_5 polymer electrolyte, one which is having 7% wt V_2O_5 shows highest photovoltaic performance. This may be due to increase in the content of V_2O_5 in the membrane which results in higher roughness, amorphous nature, increase in porosity, electrolyte uptake and ionic conductivity. This photovoltaic efficiency is comparable with that observed for PVdF-PAN-V_2O_5 composite membrane, 7.75% and is higher than that reported recently for similar systems, 0.60, 2.04, 1.66 and 2.20, 1.68 %, [52-56].

4. CONCLUSION

The PVdF-PAN- V_2O_5 nano fibrous membrane was prepared from a solution of PVdF and PAN and incorporating 3%, 5% and 7% V_2O_5 by electrospinning method. The HRSEM study shows that the PVdF-PAN-V_2O_5 fiber with 7% V_2O_5 has 264 nm diameter with three-dimensional interconnected network of regular morphology with large number of voids and cavities. The porosity percentage (84.4 – 85.9%) and electrolyte uptake (576%) increase with an increase in the V_2O_5 concentration. The ionic conductivity of PVdF-PAN-V_2O_5 fiber with 7% V_2O_5 is $7.11\times10^{-2}Scm^{-1}$. A high contact angle of 141.0° is observed for this composite fiber which shows the higher hydrophobic nature of the membrane. The prepared polymer composite membrane was soaked in the electrolyte solution and used as polymer electrolyte. Employing the polymer electrolyte, DSSCs were fabricated successfully and their photovoltaic performances were evaluated. The solar-to-light electricity conversion efficiency of the quasi-solid-state solar cells with the electrospun PVdF-PAN-V_2O_5 composite membrane electrolyte has achieved 7.75%.

ACKNOWLEDGMENTS
Mr. M. Sethupathy was thankful to UGC-BSR funding agency, India for the supporting to carry out the research. The authors acknowledge the School of Physics, Alagappa University, Karaikudi for XRD and Central Electro Chemical Research Institute (CECRI), Karaikudi for I-V measurements.

References

1. C. M. Costa, L. C. Rodrigues, V. Sencadas, M. M. Silva, J. G. Rocha, S. L. Mendez. J *Membr Sci.* 407- 408 (2012) 193-201.
2. J.S. Bonso, A. Rahy, S.D. Perera, N. Nour, O. Seitz, Y. J. Chabal, K. J. Balkus Jr, J. P. Ferraris, D. J. Yang *J Power Sources* 203 (2012) 227-232.
3. S. K. Ahn, T. Ban, P. Sakthivel, J. W. Lee, Y. S. Gal, J. K. Lee, M. R. Kim, S.H. Jin. *ACS Appl Mater Interfaces* 4 (2012) 2096-2100.
4. M. Gratzel. *J Photoch Photobio A: Chemistry* 164 (2004) 3-14.
5. S. Chuangchote, T. Sagawa, S. Yoshikawa. *Appl Phys Lett*. 93 (2008) 033310-033313.
6. A. R. Sathiya Priya, A. Subramania, Y. S. Jung, K. J. Kim. *Langmuir* 24 (2008) 9816-9819.
7. B.O. Regan, M. Gratzel. *Nature* 353 (1991) 737-740.
8. M. K. Nazeeruddin, A. Kay, I. Rodicio, R. H. Baker, E. Miiller, P. Liska, N. Vlachopoulos, M. Gratzel. *J Am Chem Soc*. 115 (1993) 6382-6390.
9. J. Doshi, D. H. Reneker. *J Electrostat*. 35 (1995) 151-160.
10. L. Feng, S. Li, H. Li, J. Zhai, Y. Song, L. Jiang, D. Zhu. *Angew Chem Int Ed*. 41 (2002) 1221-1223.
11. P. Wang, S. M. Zakeeruddin, R. H. Baker, M. Gratzel. *Chem Mater*. 16 (2004) 2694-2696.
12. S. A. Haque, E. Palomares, H. M. Upadhyaya, L. Otley, R. J. Potter, A. B. Holmes, J. R. Durrant. *Chem Commun*. 24 (2003) 3008-3009.
13. A. F. Nogueira, C. Longo, M. A. D. Paoli. *Coordin Chem* Rev. 248 (2004) 1455-1468.
14. E. Stathatos, P. Lianos, S. M. Zakeeruddin, P. Liska, M. Gratzel. *Chem Mater*. 15 (2003) 1825-1829.
15. N. Mohmeyer, P. Wang, H. W. Schmidt, S. M. Zakeeruddin, M. Gratzel. *J Mater Chem*. 14 (2004) 1905-1909.
16. Y. BokJeong, D. WonKim. *Electochim Acta*. 50 (2004) 323-326.
17. H. Huang, S. L. Wunder. *J Electrochem Society* 148 (2001) 279-283.
18. J. UnKim, S. HaePark, H. JuChoi, W. KiLee, J. KookLee, M. RaKim. *Sol Energy Mater & Sol Cells.* 93 (2009) 803-807.
19. T. Ondarcuhu, C. Joachim. *Europhys Lett*. 42 (1988) 215-220.
20. Y. L. Cheah, N. Gupta, S. S. Pramana, V. Aravindan, G. Weea, M. Srinivasan. *J Power Sources.* 196 (2011) 6465-6472.
21. J. Zeleny. *Phys Rev*. 3 (1914) 69-91.
22. A. Formhals. (1934) USPatent1975504
23. Z. M. Huang, Y. Z. Zhang, M. Kotaki, S. Ramakrichna. *Compos Sci Technol*. 63 (2003) 2223-2253.
24. J. Doshi, D. H. Reneker. *J Electrostat*. 35 (1995) 151-160.
25. S. Cavaliere, S. Subianto, I. Savych, D. J. Jones, J. Roziere. *Energ Environ Sci*. 4 (2011) 4761-4785.
26. S. Cavaliere, V. Salles, A. Brioude, Y. Lalatonne, L. Motte, P. Monod, D. Cornu, P. Miele. *J Nanopart Res.* 12 (2010) 2735-2740.
27. D. Navarathne, Y. Ner, M. Jain, J. G. Grote, G. A. Sotzing. *Mater Lett*. 65 (2011) 219-221.
28. R. Ramaseshan, S. Sundarrajan, R. Jose, S. Ramakrishna. *J Appl Phys*. 102 (2007) 111101-111117.

29. M. M. Demir, I. Yilgor, E. Yilgor, B. Erman. *Polymer* 43 (2002) 3303-3309.
30. D. H. Reneker, W. Kataphinan, A. Theron, E. Zussman, A. L. Yarin. *Polymer* 43 (2002) 6785-6794.
31. J. R. Kim, S. W. Choi, S. M. Jo, W. S. Lee, B. C. Kim. *J Electrochem Society* 152 (2005) 295.
32. A. I. Gopalan, S. Padmanabhan, K. M. Manesh, J. H. Nho, S. H. Kim, C. G. Hwang, K. P. Lee. *J Membr Sci.* 325 (2008) 683-690.
33. H. R. Junga, D. H. Jua, W. J. Leea, X. Zhang, R. Kotek. *Electrochim Acta* 54 (2009) 3630-3637.
34. L. Wang, X. He, J. Li, M. Chen, J. Gao, C. Jiang. *Electrochim Acta* 72 (2012) 114-19.
35. X .Yin, H. Cheng, X. Wang, Y. Yao. *J Membr Sci*. 146 (1998) 179-84.
36. T. Y. Liu, W. C. Lin, L. Y. Huang, S. Y. Chen, M. C. Yang. *Polym Adv Technolo*. 16 (2005) 413-19.
37. G. Rizzo, A. Arena, A. Bonavita, N. Donato, G. Neri, G. Saitta. *Thin Solid Films* 518 (2010) 7124-7127.
38. C. K. Chan, H. Peng, R. D. Twesten, K. Jarausch, X. F. Zhang, Y. Cui *Nano Lett.* 106 (2007) 490-495.
39. D. Kiriya, H. Onoe, M. Ikeda, I. Hamachi, S. Takeuchi. Proceedings in MEMS2010 (2010) 927-930.
40. C. G. Wu, D. C. DeGroot, H. O. Marcy, J. L. Schindler, C. R. Kannewurf, Y. J. Liu, W. Hirpo, M. G. Kanatzidis. *Chem Mater*. 8 (1996) 1992-2004.
41. J. Livage. *Chem Mater*. 3 (1991) 578-593.
42. R. A. Zoppi, C. G. A. Soares. *Adv Polym Technol.* 21 (2002) 2-16.
43. M. Wachtler, D. Ostrovskii, P. Jacobsson, B. Scrosati. *Electrochim Acta* 50 (2004) 357-361.
44. E. Lugscheider, K. Bobzin. *Surf Coat Tech.* 165 (2003) 51- 57.
45. Z. L. Xu, F. A. Qusay. *J Appl Polym Sci*. 91 (2004) 3398-3407.
46. H. R. Jung, D. H. Ju, W. J. Lee, X. Zhang, R. Kotek. *Electrochim Acta* 54 (2009) 3630-3637.
47. A. V. R. Reddy, D. J. Mohan, A. Bhattacharya, V. Shah, P. K. Ghosh. *J Membr Sci*. 214 (2003) 211-221.
48. A. Taniguchi, M. Cakmak. *Polymer* 45 (2004) 6647-6654.
49. J. K. Lee, H. J. Choi, S. H. Park, D. H. Won, H. W. Park, J. H. Kim, C. J. Lee, S. H. Jeong, M. R. Kim. *Mol Cryst Liq Cryst*. 519 (2010) 234-44.
50. J. K. Kim, G. Cheruvally, X. Li, J. H. Ahn, K. W. Kim, H. J. Ahn. *J Power Sources* 178 (2008) 815-820.
51. Y. Yang, J. Zhang, C. Zhou, S. Wu, S. Xu, W. Liu, H. Han, B. Chen, X. Z. Zhao. *J Phys Chem* B. 112 (2008) 6594-6602.
52. P. K. Singh, K. I. Kim, N. G. Park, H. W. Rhee *Macromol Symp*. 249-250 (2007) 162-166.
53. G. P. Kalaignan, M. S. Kang, Y. S. Kang. *J Solid State Ionics* 177 (2006) 1091-1097.
54. J. H. Kim, M. S. Kang, Y. J. Kim, J. Won, Y. S. Kang. *J Solid State Ionics* 176 (2005) 579-584.
55. M. M. Noor, M. H. Buraldah, S. N. F. Yusuf, M. A. Careem, S. R. Majid, A. K. Arof *Int. J. Photoenergy* (2011) 1-5.
56. P. K. Singh, B. Bhattacharya, R. K. Nagarale. *J Appl Polym Sci*. 118 (2010) 2976-2980.